Journal of Applied Fluid Mechanics, Vol. 8, No. 1, pp. 7-20, 2015.
Available online at www.jafmonline.net, ISSN 1735-3572, EISSN 1735-3645.
DOI: 10.36884/jafm.8.01.22600

Natural Convection Heat and Mass Transfer Flow with Hall Current, Rotation, Radiation and Heat Absorption Past an Accelerated Moving Vertical Plate with Ramped Temperature

G. S. Seth†, R. Sharma and S. Sarkar

Department of Applied Mathematics, Indian School of Mines, Dhanbad 826004, India.

†*Corresponding Author Email: gsseth_ism@yahoo.com, gsseth.ism@gmail.com*

(Received December 23, 2013; accepted January 4, 2014)

ABSTRACT

An investigation of unsteady hydromagnetic natural convection heat and mass transfer flow with Hall current of a viscous, incompressible, electrically conducting, heat absorbing and optically thin radiating fluid past an accelerated moving vertical plate through fluid saturated porous medium in a rotating environment is carried out when temperature of the plate has a temporarily ramped profile. The exact solutions of momentum, energy and concentration equations are obtained in closed form by Laplace transform technique. The expressions of skin friction, Nusselt number and Sherwood number are also derived. For both ramped temperature and isothermal plates, Hall current tends to accelerate primary and secondary fluid velocities whereas heat absorption and radiation have reverse effect on it. Rotation tends to retard primary fluid velocity whereas it has a reverse effect on secondary fluid velocity. Heat absorption and radiation have tendency to enhance rate of heat transfer at the plate.

Keywords: Hall current, Coriolis force, Ramped temperature, Heat absorption and Thermal radiation.

NOMENCLATURE

a^*	absorption coefficient
B_0	uniform magnetic field
C'	species concentration
c_p	specific heat at constant pressure
D_M	chemical molecular diffusivity
g	acceleration due to gravity
G_r	thermal Grashof number
G_c	solutal Grashof number
k	thermal conductivity of the fluid
K_1'	permeability of porous medium
K_1	permeability parameter
K^2	rotation parameter
m	Hall current parameter
M	magnetic parameter
R	radiation parameter
P_r	Prandtl number
Q_0	heat absorption coefficient
q_r'	radiating flux vector
S_c	Schmidt number
T'	fluid temperature
t_0	characteristic time
U_0	characteristic velocity
u'	fluid velocity in x' direction
w'	fluid velocity in z' direction

Greek Symbols

β'	coefficient of thermal expansion
Ω	uniform angular velocity
β^*	coefficient of expansion for species concentration
σ	electrical conductivity
ρ	fluid density
σ^*	Stefan-Boltzmann constant
ν	kinematic coefficient of viscosity
ω_e	cyclotron frequency
τ_e	electron collision time
ϕ	heat absorption parameter

1. INTRODUCTION

Heat absorption/generation effects play a significant role on the heat transfer characteristics of several physical problems of practical interest viz. convection in Earth's mantle, post-accident heat removal, fire and combustion modeling, fluids undergoing exothermic and/or endothermic chemical reaction, development of metal waste from spent nuclear fuel, applications in the field of nuclear energy etc. Therefore, it is appropriate to consider temperature dependent heat source and/or sink which may have strong influence on heat and mass transfer characteristics of the fluid flow problems under consideration. However, exact mathematical modeling of internal heat generation/absorption is highly complicated. It is noticed that some simple mathematical models yet idealized may express their average behavior for most of the physical situations. Sparrow and Cess (1961) were one of the initial investigators to consider temperature dependent heat absorption on steady stagnation point flow and heat transfer. Later, several researchers considered hydromagnetic natural convection flow past a flat plate considering different aspects of the problem. Mention may be made of the research studies of Chamkha and Khaled (2001), Chamkha (2004), Ramadan and Chamkha (2004) and Das et al. (2009). Jha and Ajibade (2009) analyzed natural convection flow of a temperature dependent heat generating/absorbing fluid between vertical porous plates with periodic heat input. Thermal radiation in hydromagnetic flows is an essential aspect of various scenarios in aerospace, mechanical, chemical, environmental and hazards engineering. Industrial applications such as glass production and furnace design, space technology applications such as cosmical flight aerodynamics, rocket propulsion systems and spacecraft re-entry vehicles operate at high temperatures where radiation effects are greatly significant. It is worthy to note that unlike convection/conduction the governing equations considering the effects of radiation become quite complicated due to the inclusion of radiation term in the energy equation making it nonlinear. Some reasonable approximations are proposed to solve the governing equations with radiative heat transfer. England and Emery (1969) investigated the effects of thermal radiation on laminar free convection boundary layer flow past a vertical plate for heat absorbing and non absorbing gases. They obtained velocity and temperature profiles experimentally for constant heat flux boundary condition in case of air and carbon-dioxide and these were compared with analytical solutions for optically thin gases and absorbing gray gases. Hossain and Takhar (1996) studied the effects of radiation on mixed convection boundary layer flow near a vertical plate with uniform surface temperature using Rosseland flux model. Contributions are also due to Azzam (2002), Raptis et al. (2003), Ogulu and Prakash (2006), Raptis (2011), Reddy et al. (2013), Prakash et al. (2013). Moreover, the combined effects of thermal radiation and heat generation/absorption on hydromagnetic natural convection flow play a crucial role in controlling the heat transfer and may have promising applications in the industry. Keeping in view the importance of such study, Chamkha (2000) studied thermal radiation and buoyancy effects on hydromagnetic flow over an accelerating permeable surface with heat source or sink. Seddeek (2001) investigated thermal radiation and buoyancy effects on MHD natural convection heat generating flow past an accelerating permeable surface with temperature-dependent viscosity. Saha et al. (2010) considered the combined effects of thermal radiation and heat generation on hydromagnetic flow past a uniformly heated vertical plate. Prasad et al. (2013) investigated the effects of internal heat generation/absorption, thermal radiation, magnetic field and temperature dependent thermal conductivity on the flow and heat transfer characteristics of a Non-Newtonian Maxwell fluid over a stretching sheet.

Several investigations on natural convection flows are performed using both analytical and numerical methods under different thermal conditions which are continuous and well-defined. However, practical problems often involve thermal conditions which may be non-uniform or arbitrary. Some of the numerous industry based applications considering non-uniform thermal conditions include nuclear heat transfer control, materials processing, turbine blade heat transfer, electronic circuits and sealed gas-filled enclosure heat transfer operations. Narahari et al. (2011) considered flow of a viscous incompressible fluid past an infinite vertical plate with ramped temperature taking into account the presence of foreign mass or constant mass flux. Patra et al. (2012) considered the effects of radiation on natural convection flow of a viscous and incompressible fluid near a stationary vertical flat plate with ramped temperature. Nandkeolyar et al. (2013a) investigated unsteady hydromagnetic natural convection flow of a dusty fluid past an impulsively moving vertical plate with ramped temperature in the presence of thermal radiation. Subsequently, Nandkeolyar et al. (2013b) considered unsteady hydromagnetic heat and mass transfer flow of a heat radiating and chemically reactive fluid past a flat porous plate with ramped wall temperature. Contributions are also due to Nandkeolyar and Das (2013) and Nandkeolyar et al. (2013c).

Study of hydromagnetic natural convection flow in a rotating medium has great significance due to its applications in many areas of geophysics, astrophysics and fluid engineering. Taking into account of this fact, Singh (1983), Nanousis (1992), Singh et al. (2010) investigated unsteady hydromagnetic natural convection flow past a flat plate in a rotating medium considering different aspects of the problem. Seth et al. (2011) considered the effects of rotation on unsteady hydromagnetic natural convection flow past an impulsively moving vertical plate with ramped temperature in a porous medium with thermal diffusion and heat absorption. Ghosh et al. (2013) studied unsteady hydromagnetic mixed convection flow in a rotating channel subject to forced oscillation under an oblique magnetic field.

Muthucumaraswamy et al. (2013) considered the effects of rotation on unsteady hydromagnetic natural convection flow past an uniformly accelerated isothermal infinite vertical plate with variable mass diffusion in the presence of chemical reaction of first order. Seth et al. (2013b) analyzed the effects of thermal radiation and rotation on unsteady hydromagnetic free convection flow past an impulsively moving vertical plate embedded in porous medium with ramped temperature.

It is noticed that when the density of an electrically conducting fluid is low and/or applied magnetic field is strong, Hall current plays a vital role in determining flow-features of the fluid flow problems because it induces secondary flow in the flow-field (Sutton and Sherman (1965). Taking into account of this fact, Aboeldahab and Elbarbary (2001) and Seth et al. (2012) investigated the effects of Hall current on hydromagnetic free convection boundary layer flow past a flat plate considering different aspects of the problem. It is noteworthy that Hall current induces secondary flow in the flow-field which is also the characteristics of Coriolis force. Therefore, it is essential to compare and contrast the effects of these two agencies and also to study their combined effects on such fluid flow problems. Narayana et al. (2013) studied the effects of Hall current and radiation-absorption on MHD natural convection heat and mass transfer flow of a micropolar fluid in a rotating frame of reference. Recently, Seth et al. (2013a) investigated the effects of Hall current and rotation on unsteady hydromagnetic natural convection flow of a viscous, incompressible, electrically conducting and heat absorbing fluid past an impulsively moving vertical plate with ramped temperature in a porous medium taking into account the effects of thermal diffusion.

Aim of the present investigation is to study unsteady hydromagnetic natural convection heat and mass transfer flow with Hall current of a viscous, incompressible, electrically conducting, temperature dependent heat absorbing and optically thin heat radiating fluid past an accelerated moving vertical plate through fluid saturated porous medium in a rotating environment when temperature of the plate has a temporarily ramped profile. This problem has not yet received any attention from the researchers although natural convection heat and mass transfer flow of a heat absorbing and radiating fluid resulting from such ramped temperature profile of a plate moving with time dependent velocity may have strong bearings on numerous problems of practical interest where initial temperature profiles are of much significance in designing of so many hydromagnetic devices and in several industrial processes occurring at high temperatures where the effects of thermal radiation and heat absorption play a vital role in the fluid flow characteristics.

2. FORMULATION of THE PROBLEM and its SOLUTION

Consider unsteady hydromagnetic natural convection flow of an electrically conducting, viscous, incompressible and temperature dependent heat absorbing and optically thin heat radiating fluid past a infinite moving vertical plate embedded in a porous medium taking Hall effects into account. Choose the coordinate system in such a way that x'-axis is along the length of the plate in the upward direction and y'-axis normal to the plane of the plate in the fluid. A uniform transverse magnetic field B_0 is applied parallel to y'-axis. Both the fluid and plate are in rigid body rotation with uniform angular velocity Ω about y'-axis. Initially i.e. at time $t' \le 0$, both the fluid and plate are at rest and at uniform temperature T'_∞. Also species concentration within the fluid is maintained at uniform concentration C'_∞. At time $t' > 0$, plate starts moving with time dependent velocity $U(t')$ in x' direction and temperature of the plate is raised or lowered to $T'_\infty + (T'_w - T'_\infty)t'/t_0$ when $t' \le t_0$, and thereafter, i.e. at $t' > t_0$, plate is maintained at uniform temperature T'_w. Also, at time $t' > 0$, species concentration at the surface of the plate is raised to uniform species concentration C'_w and is maintained thereafter. Geometry of the problem is presented in Fig. 1. Since plate is of infinite extent along x' and z' directions and is electrically non-conducting, all physical quantities, depend on y' and t' only. It is assumed that the induced magnetic field produced by fluid motion is negligible in comparison to the applied one. This assumption is valid because magnetic Reynolds number is very small for metallic liquids and partially ionized fluids (Cramer and Pai, 1973). Also no external electric field is applied so the effects of polarization of fluid is negligible (Cramer and Pai, 1973).

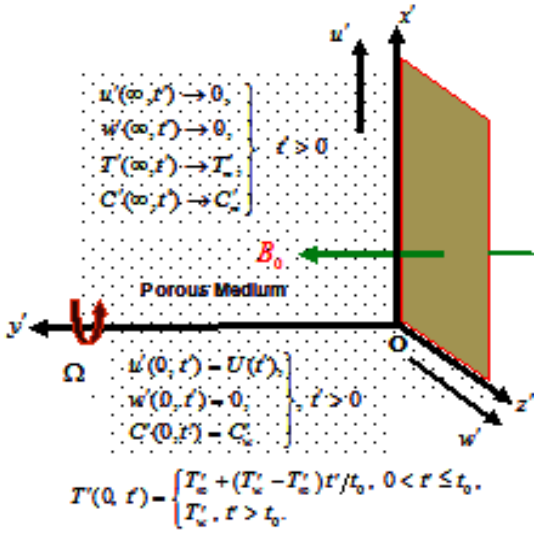

Fig. 1. Geometry of the Problem

Keeping in view of the assumptions made above, the governing equations for unsteady hydromagnetic natural convection flow of a viscous, incompressible, electrically conducting and temperature dependent heat absorbing and optically thin heat radiating fluid in a uniform porous medium taking Hall effects and rotation into account are given by

$$\frac{\partial u'}{\partial t'} + 2\Omega w' = \nu \frac{\partial^2 u'}{\partial y'^2} - \left(\frac{\sigma B_0^2}{\rho}\right)\frac{(u' + mw')}{(1+m^2)} - \nu \frac{u'}{K_1'} + g\beta'(T' - T_\infty') + g\beta^*\left(C' - C_\infty'\right), \quad (1)$$

$$\frac{\partial w'}{\partial t'} - 2\Omega u' = \nu \frac{\partial^2 w'}{\partial y'^2} + \left(\frac{\sigma B_0^2}{\rho}\right)\frac{(mu' - w')}{(1+m^2)} - \nu \frac{w'}{K_1'}, \quad (2)$$

$$\frac{\partial T'}{\partial t'} = \frac{k}{\rho c_p}\frac{\partial^2 T'}{\partial y'^2} - \frac{Q_0}{\rho c_p}(T' - T_\infty') - \frac{1}{\rho c_p}\frac{\partial q_r'}{\partial y'}, \quad (3)$$

$$\frac{\partial C'}{\partial t'} = D_M \frac{\partial^2 C'}{\partial y'^2}, \quad (4)$$

where $m = \omega_e \tau_e$ is Hall current parameter.

u', w', T', K_1', k, c_p, Q_0, C', D_M, q_r', ν, σ, ρ, g, β', β^*, ω_e and τ_e are, respectively, fluid velocity in x'– direction, fluid velocity along $z'-$ direction, fluid temperature, permeability of porous medium, thermal conductivity, specific heat at constant pressure, heat absorption coefficient, species concentration, chemical molecular diffusivity, radiating flux vector, kinematic coefficient of viscosity, electrical conductivity, fluid density, acceleration due to gravity, coefficient of thermal expansion, coefficient of expansion for species concentration, cyclotron frequency and electron collision time.

Initial and boundary conditions for the fluid flow problem are given below

$$u' = w' = 0,\ T' = T_\infty',\ C' = C_\infty',\ \text{for } y' \geq 0 \text{ and } t' \leq 0, \quad (5a)$$

$$u' = U(t'),\ w' = 0,\ C' = C' \text{ at } y' = 0 \text{ for } t' > 0, \quad (5b)$$

$$T' = T_\infty' + (T_w' - T_\infty')t'/t_0 \text{ at } y' = 0 \text{ for } 0 < t' \leq t_0, \quad (5c)$$

$$T' = T_w' \text{ at } y' = 0 \text{ for } t' > t_0, \quad (5d)$$

$$u',\ w' \to 0, T' \to T_\infty', C' \to C_\infty' \text{ as } y' \to \infty \text{ for } t' > 0. \quad (5e)$$

In the case of an optically thin gray fluid the local radiant absorption (Raptis, 2011) is expressed as:

$$\frac{\partial q_r'}{\partial y'} = -4a^*\sigma^*\left(T_\infty'^4 - T'^4\right), \quad (6)$$

where a^* is absorption coefficient and σ^* is Stefan-Boltzmann constant.

It is assumed that the temperature difference within the fluid flow is sufficiently small such that fluid temperature T'^4 may be expressed as a linear function of the temperature. This is accomplished by expanding T'^4 in a Taylor series about free stream temperature T_∞'. Neglecting second and higher order terms, T'^4 is expressed as

$$T'^4 \cong 4T_\infty'^3 T' - 3T_\infty'^4. \quad (7)$$

Making use of Eqs. (6) and (7) in Eq. (3), we obtain

$$\frac{\partial T'}{\partial t'} = \frac{k}{\rho c_p}\frac{\partial^2 T'}{\partial y'^2} - \frac{16a^*\sigma^* T_\infty'^3}{\rho c_p}(T' - T_\infty') - \frac{Q_0}{\rho c_p}(T' - T_\infty'). \quad (8)$$

Introducing non-dimensional variables and parameters

$$y = y'/U_0 t_0,\ u = u'/U_0,\ w = w'/U_0,\ t = t'/t_0,$$

$$T = (T' - T_\infty')/(T_w' - T_\infty'),\ C = \left(C' - C_\infty'\right)/\left(C_w' - C_\infty'\right),$$

$$M = \sigma B_0^2 \nu/\rho U_0^2,\ K^2 = \Omega\nu/U_0^2,\ K_1 = K_1' U_0^2/\nu^2,$$

$$G_r = g\beta'\nu(T_w' - T_\infty')/U_0^3,\ G_c = \nu g\beta^*\left(C_w' - C_\infty'\right)/U_0^3,$$

$$P_r = \nu\rho c_p/k,\ \phi = \nu Q_0/\rho c_p U_0^2,$$

$$R = 16a^*\sigma\nu T_\infty'/U_0^2\rho c_p \text{ and } S_c = \nu/D_M. \quad (9)$$

Equations (1), (2), (4) and (8), in non-dimensional form, become

$$\frac{\partial u}{\partial t} + 2K^2 w = \frac{\partial^2 u}{\partial y^2} - \frac{M\left(u + mw\right)}{\left(1+m^2\right)} - \frac{u}{K_1} + G_r T + G_c C, \quad (10)$$

$$\frac{\partial w}{\partial t} - 2K^2 u = \frac{\partial^2 w}{\partial y^2} + \frac{M\left(mu - w\right)}{\left(1+m^2\right)} - \frac{w}{K_1}, \quad (11)$$

$$\frac{\partial T}{\partial t} = \frac{1}{P_r}\frac{\partial^2 T}{\partial y^2} - RT - \phi T, \quad (12)$$

$$\frac{\partial C}{\partial t} = \frac{1}{S_c}\frac{\partial^2 C}{\partial y^2}, \quad (13)$$

where K^2, M, K_1, G_r, G_c, P_r, R, ϕ and S_c are, respectively, rotation parameter, magnetic parameter, permeability parameter, thermal Grashof number, solutal Grashof number, Prandtl number, radiation parameter, heat absorption parameter and Schmidt number.

It may be noted that characteristic time t_0 may be defined according to the non-dimensional process mentioned above as

$$t_0 = \nu/U_0^2, \quad (14)$$

where U_0 is characteristic velocity.

Initial and boundary conditions, presented by Eqs. (5a) to (5e), in non-dimensional form, are given by

$$u = w = 0,\ T = 0,\ C = 0 \text{ for } y \geq 0 \text{ and } t \leq 0, \quad (15a)$$

$$u = f(t),\ w = 0,\ C = 1 \text{ at } y = 0 \text{ for } t > 0, \quad (15b)$$

$$T = t \text{ at } y = 0 \text{ for } 0 < t \leq 1, \quad (15c)$$

$$T = 1 \text{ at } y = 0 \text{ for } t > 1, \quad (15d)$$

$$u,\ w \to 0,\ T \to 0,\ C \to 0 \text{ as } y \to \infty \text{ for } t > 0, \quad (15e)$$

where $f(t) = U(t')/U_0$.

Combining Eqs. (10) and (11), we obtain

$$\frac{\partial F}{\partial t} - 2iK^2F = \frac{\partial^2 F}{\partial y^2} - NF - \frac{F}{K_1} + G_r T + G_c C, \qquad (16)$$

where $F = u + iw$ and $N = M/(1+im)$.

Initial and boundary conditions, presented by Eqs. (15a) to (15e), in compact form, are given by

$$F = 0, T = 0, C = 0 \quad \text{for } y \geq 0 \text{ and } t \leq 0, \qquad (17a)$$

$$F = f(t),\ C = 1 \quad \text{at } y = 0 \text{ for } t > 0, \qquad (17b)$$

$$T = t \quad \text{at } y = 0 \text{ for } 0 < t \leq 1, \qquad (17c)$$

$$T = 1 \quad \text{at } y = 0 \text{ for } t > 1, \qquad (17d)$$

$$F \to 0, T \to 0, C \to 0 \quad \text{as } y \to \infty \text{ for } t > 0. \qquad (17e)$$

In order to investigate the flow features of the fluid flow generated due to uniformly accelerated movement of the plate, we consider $f(t) = R_1 t$ where R_1 is a non-dimensional constant.

Using Laplace transform technique in Eqs. (12), (13) and (16), exact solutions for fluid temperature $T(y,t)$, species concentration $C(y,t)$ and fluid velocity $F(y,t)$ are obtained and are presented in the following form after simplification.

$$T(y,t) = P(y,t) - H(t-1)P(y,t-1), \qquad (18)$$

$$C = erfc\left(\frac{y\sqrt{S_c}}{2\sqrt{t}}\right), \qquad (19)$$

$$\begin{aligned} F(y,t) = G(y,t) + H(t-1)G(y,t-1) + \frac{R_1}{2}\Bigg[\left(t + \frac{y}{2\sqrt{\beta_1}}\right)\times \\ e^{y\sqrt{\beta_1}}erfc\left(\frac{y}{2\sqrt{t}} + \sqrt{\beta_1 t}\right) + \left(t - \frac{y}{2\sqrt{\beta_1}}\right)e^{-y\sqrt{\beta_1}}\times \\ erfc\left(\frac{y}{2\sqrt{t}} - \sqrt{\beta_1 t}\right) + \frac{\gamma}{2b}\Bigg[e^{bt}\Bigg\{e^{y\sqrt{(\beta_1+b)}}\times \\ erfc\left(\sqrt{(\beta_1+b)t} + \frac{y}{2\sqrt{t}}\right) + e^{-y\sqrt{(\beta_1+b)}}\times \\ erfc\left(\frac{y}{2\sqrt{t}} - \sqrt{(\beta_1+b)t}\right) - e^{y\sqrt{S_c b}}\times \\ erfc\left(\sqrt{bt} + \frac{y}{2}\sqrt{\frac{S_c}{t}}\right) - e^{-y\sqrt{S_c b}}\times \\ erfc\left(\frac{y}{2}\sqrt{\frac{S_c}{t}} - \sqrt{bt}\right)\Bigg\} - \Bigg\{e^{y\sqrt{\beta_1}}\times \\ erfc\left(\sqrt{\beta_1 t} + \frac{y}{2\sqrt{t}}\right) + e^{-y\sqrt{\beta_1}} \\ erfc\left(\frac{y}{2\sqrt{t}} - \sqrt{\beta_1 t}\right) - 2erfc\left(\frac{y}{2}\sqrt{\frac{S_c}{t}}\right)\Bigg], \end{aligned} \qquad (20)$$

$$\begin{aligned} P(y,t) = \frac{1}{2}\Bigg[e^{y\sqrt{P_r\beta_2}}erfc\left(\sqrt{\beta_2 t} + \frac{y}{2}\sqrt{\frac{P_r}{t}}\right)\left(t + \frac{y}{2}\sqrt{\frac{P_r}{\beta_2}}\right) \\ + e^{-y\sqrt{P_r\beta_2}}erfc\left(\frac{y}{2}\sqrt{\frac{P_r}{t}} - \sqrt{\beta_2 t}\right)\left(t - \frac{y}{2}\sqrt{\frac{P_r}{\beta_2}}\right)\Bigg], \end{aligned}$$

$$\begin{aligned} G(y,t) = \frac{\alpha}{2a^2}\Bigg[e^{at}\{-e^{y\sqrt{(\beta_1+a)}}erfc\left(\sqrt{(\beta_1+a)t} + \frac{y}{2\sqrt{t}}\right) \\ -e^{-y\sqrt{(\beta_1+a)}}erfc\left(-\sqrt{(\beta_1+a)t} + \frac{y}{2\sqrt{t}}\right) + \\ e^{y\sqrt{P_r(\beta_2+a)}}erfc\left(\sqrt{(\beta_2+a)t} + \frac{y}{2}\sqrt{\frac{P_r}{t}}\right) + \\ e^{-y\sqrt{P_r(\beta_2+a)}}erfc\left(-\sqrt{(\beta_2+a)t} + \frac{y}{2}\sqrt{\frac{P_r}{t}}\right) \\ -a\Bigg\{-e^{y\sqrt{\beta_1}}erfc\left(\sqrt{\beta_1 t} + \frac{y}{2\sqrt{t}}\right)\left(\frac{1}{a} + t + \right. \\ \left. + \frac{y}{2\sqrt{\beta_1}}\right) - e^{-y\sqrt{\beta_1}}erfc\left(-\sqrt{\beta_1 t} + \frac{y}{2\sqrt{t}}\right)\left(\frac{1}{a} + \right. \\ \left. t - \frac{y}{2\sqrt{\beta_1}}\right) + e^{y\sqrt{P_r\beta_2}}erfc\left(\frac{y}{2}\sqrt{\frac{P_r}{t}} + \sqrt{\beta_2 t}\right) \\ \left(\frac{1}{a} + t + \frac{y\sqrt{P_r}}{2\sqrt{\beta_2}}\right) + e^{-y\sqrt{P_r\beta_2}}erfc\left(\frac{y}{2}\sqrt{\frac{P_r}{t}} - \right. \\ \left. -\sqrt{\beta_2 t}\right)\left(\frac{1}{a} + t - \frac{y}{2}\sqrt{\frac{P_r}{\beta_2}}\right)\Bigg\}\Bigg], \end{aligned}$$

where $H(t-1)$ and $erfc(x)$ are, respectively, unit step function and complementary error function, $\beta_1 = N + 1/K_1 - 2iK^2$, $\beta_2 = R + \phi$, $a = \dfrac{(P_r\beta_2 - \beta_1)}{(1-P_r)}$, $b = \beta_1/(S_c - 1)$, $\alpha = G_r/(1-P_r)$, $\gamma = G_c/(S_c - 1)$.

2.1 Solution for Unit Prandtl and Unit Schmidt Number

It may be noted that the solution, presented by Eq. (20) for fluid_velocity $F(y,t)$ is not valid for unit Prandtl number and unit Schmidt number. Since Prandtl number is a measure of the relative strength of viscosity to thermal diffusivity of fluid and Schmidt number is a measure of the relative strength of viscosity to molecular (mass) diffusivity of fluid, the case $P_r = 1$ and $S_c = 1$ corresponds to those fluids for which the viscous, thermal and concentration boundary layer thicknesses are same order of magnitude. There are some fluids of practical significance which belong to this category (Chen, 2004). Setting $P_r = 1$ and $S_c = 1$ in Eqs. (12) and (13) and following the same procedure adopted earlier, exact solutions for fluid temperature $T(y,t)$, fluid concentration $C(y,t)$ and fluid velocity $F(y,t)$ are obtained and are presented in the following form

$$T(y,t)=P_1(y,t)-H(t-1)P_1(y,t-1), \tag{21}$$

$$C=erfc\left(\frac{y}{2\sqrt{t}}\right), \tag{22}$$

$$F=\frac{R_1}{2}\left[\left(t+\frac{y}{2\sqrt{\beta_1}}\right)e^{y\sqrt{\beta_1}}erfc\left(\frac{y}{2\sqrt{t}}+\sqrt{\beta_1 t}\right)+\left(t-\frac{y}{2\sqrt{\beta_1}}\right)e^{-y\sqrt{\beta_1}}erfc\left(\frac{y}{2\sqrt{t}}-\sqrt{\beta_1 t}\right)\right]+\frac{b_1}{2}\left[-e^{y\sqrt{\beta_1}}erfc\left(\sqrt{\beta_1 t}+\frac{y}{2\sqrt{t}}\right)-e^{-y\sqrt{\beta_1}}\times erfc\left(\frac{y}{2\sqrt{t}}-\sqrt{\beta_1 t}\right)+2erfc\left(\frac{y}{2\sqrt{t}}\right)\right]+G_1(y,t)-H(t-1)G_1(y,t-1), \tag{23}$$

where

$$P_2(y.t)=\frac{1}{2}\left[\left(t+\frac{y}{2\sqrt{\beta_2}}\right)e^{y\sqrt{\beta_2}}erfc\left(\frac{y}{2\sqrt{t}}+\sqrt{\beta_2 t}\right)+\left[\left(t-\frac{y}{2\sqrt{\beta_2}}\right)e^{-y\sqrt{\beta_2}}erfc\left(\frac{y}{2\sqrt{t}}-\sqrt{\beta_2 t}\right)\right],$$

$$G_1(y,t)=\left(\frac{a_1}{2}\right)\left[\left(t+\frac{y}{2\sqrt{\beta_1}}\right)e^{y\sqrt{\beta_1}}erfc\left(\frac{y}{2\sqrt{t}}+\sqrt{\beta_1 t}\right)+\left(t-\frac{y}{2\sqrt{\beta_1}}\right)e^{-y\sqrt{\beta_1}}erfc\left(\frac{y}{2\sqrt{t}}-\sqrt{\beta_1 t}\right)-\left(t+\frac{y}{2\sqrt{\beta_2}}\right)e^{y\sqrt{\beta_2}}erfc\left(\frac{y}{2\sqrt{t}}+\sqrt{\beta_2 t}\right)-\left(t-\frac{y}{2\sqrt{\beta_2}}\right)e^{-y\sqrt{\beta_2}}erfc\left(\frac{y}{2\sqrt{t}}-\sqrt{\beta_2 t}\right)\right],$$

where $a_1=G_r/(\beta_2-\beta_1)$ and $b_1=G_c/\beta_1$.

2.2 Solution when Fluid is in Contact to Isothermal Plate

Analytical solution, presented by Eqs. (18) and (20), is solution for fluid temperature and fluid velocity for the flow of an electrically conducting, viscous, incompressible, temperature dependent heat absorbing and radiating fluid past an accelerated moving vertical plate in a rotating medium with ramped temperature taking Hall effects into account. In order to emphasize the effects of ramped temperature distribution within the plate on fluid flow, it may be justified to compare such a flow with the one past an accelerated moving vertical plate with uniform temperature. Keeping in view the assumptions made earlier, the solution for fluid temperature and fluid velocity for the flow past an accelerated moving and rotating isothermal vertical plate is obtained and is presented in the following form

$$T(y,t)=\frac{1}{2}\left[e^{y\sqrt{P_r\beta_2}}erfc\left(\sqrt{\beta_2 t}+\frac{y}{2}\sqrt{\frac{P_r}{t}}\right)+e^{-y\sqrt{P_r\beta_2}}\times erfc\left(\frac{y}{2}\sqrt{\frac{P_r}{t}}-\sqrt{\beta_2 t}\right)\right] \tag{24}$$

$$F=\frac{R_1}{2}\left[\left(t+\frac{y}{2\sqrt{\beta_1}}\right)e^{y\sqrt{\beta_1}}erfc\left(\frac{y}{2\sqrt{t}}+\sqrt{\beta_1 t}\right)+\left(t-\frac{y}{2\sqrt{\beta_1}}\right)e^{-y\sqrt{\beta_1}}erfc\left(\frac{y}{2\sqrt{t}}-\sqrt{\beta_1 t}\right)\right]+\left(\frac{\alpha}{2a}\right)\left[e^{at}\left\{-e^{y\sqrt{(\beta_1+a)}}erfc\left(-\sqrt{(\beta_1+a)t}+\frac{y}{2\sqrt{t}}\right)-e^{-y\sqrt{(\beta_1+a)}}erfc\left(-\sqrt{(\beta_1+a)t}+\frac{y}{2\sqrt{t}}\right)+e^{y\sqrt{P_r(\beta_2+a)}}\times erfc\left(\sqrt{(\beta_2+a)t}+\frac{y}{2}\sqrt{\frac{P_r}{t}}\right)+e^{-y\sqrt{P_r(\beta_2+a)}}\times erfc\left(-\sqrt{(\beta_2+a)t}+\frac{y}{2}\sqrt{\frac{P_r}{t}}\right)\right\}+e^{y\sqrt{\beta_1}}\times erfc\left(\sqrt{\beta_1 t}+\frac{y}{2\sqrt{t}}\right)+e^{-y\sqrt{\beta_1}}erfc\left(-\sqrt{\beta_1 t}+\frac{y}{2\sqrt{t}}\right)-e^{y\sqrt{P_r\beta_2}}erfc\left(\sqrt{\beta_2 t}+\frac{y}{2}\sqrt{\frac{p_r}{t}}\right)-e^{-y\sqrt{P_r\beta_2}}erfc\left(-\sqrt{\beta_2 t}+\frac{y\sqrt{P_r}}{2\sqrt{t}}\right)+\frac{\gamma}{2b}\left[e^{bt}\left\{e^{y\sqrt{(\beta_1+b)}}erfc\left(\sqrt{(\beta_1+b)t}+\frac{y}{2\sqrt{t}}\right)+e^{-y\sqrt{(\beta_1+b)}}erfc\left(-\sqrt{(\beta_1+b)t}+\frac{y}{2\sqrt{t}}\right)-e^{y\sqrt{S_c b}}\times erfc\left(\sqrt{bt}+\frac{y}{2}\sqrt{\frac{S_c}{t}}\right)-e^{-y\sqrt{S_c b}}erfc\left(-\sqrt{bt}+\frac{y}{2}\sqrt{\frac{S_c}{t}}\right)\right\}+\left\{-e^{y\sqrt{\beta_1}}erfc\left(\sqrt{\beta_1 t}+\frac{y}{2\sqrt{t}}\right)-e^{-y\sqrt{\beta_1}}erfc\left(-\sqrt{\beta_1 t}+\frac{y}{2\sqrt{t}}\right)+2erf\,c\left(\frac{y}{2}\sqrt{\frac{S_c}{t}}\right)\right\}\right]. \tag{25}$$

2.3 Skin Friction and Nusselt Number

Expressions for primary skin friction τ_x, secondary skin friction τ_z and Nusselt number N_u, which are measures of shear stress at the plate due to primary flow, shear stress at the plate due to secondary flow and rate of heat transfer at the plate respectively, are presented in the following form for ramped temperature and isothermal plates.

(i) For ramped temperature plate

$$\tau=\tau_x+i\tau_z=\frac{R_1}{2}\left[\left(\frac{1}{\sqrt{\beta_1}}+2t\sqrt{\beta_1}\right)\left(erfc\left(\sqrt{\beta_1 t}\right)-1\right)-2\sqrt{\frac{t}{\pi}}e^{-\beta_1 t}\right]+\frac{\gamma}{2b}\left[e^{bt}\left\{2\sqrt{(\beta_1+b)}\times\left(erfc\left(\sqrt{(\beta_1+b)t}\right)-1\right)-2\sqrt{S_c b}\left(erfc\left(\sqrt{bt}\right)-1\right)\right.\right.$$

$$-2\sqrt{\beta_1}\left(erfc\left(\sqrt{\beta_1 t}\right)-1\right)\Big]+G_2(y,t)+$$
$$H(t-1)G_2(y,t-1), \quad (26)$$

$$N_u = P_2(y,t)-H(t-1)P_2(y,t-1), \quad (27)$$

Where

$$G_2(y,t)=\frac{\alpha}{2a^2}\Big[e^{at}\left\{-2\sqrt{(\beta_1+a)}\left(erfc\left(\sqrt{(\beta_1+a)t}\right)-1\right)+ 2\sqrt{P_r(\beta_2+a)}\left(erfc\left(\sqrt{(\beta_2+a)t}\right)-1\right)+ \frac{2}{\sqrt{t\pi}}e^{-(\beta_1+a)t}-\frac{2\sqrt{P_r}}{\sqrt{t\pi}}e^{-(\beta_2+a)t}\right\}-a\left\{-\left(\frac{1}{\beta_1}+2\sqrt{\beta_1}\left(t+\frac{1}{a}\right)\right)\left(erfc\left(\sqrt{\beta_1 t}\right)-1\right)+\left(erfc\left(\sqrt{\beta_2 t}\right)-1\right)\times \left(2\sqrt{\beta_2 P_r}\left(t+\frac{1}{a}\right)+\sqrt{\frac{P_r}{\beta_2}}\right)+2\left(t+\frac{1}{a}\right)\frac{1}{\sqrt{t\pi}}\times e^{-\beta_1 t}-2\sqrt{\frac{P_r}{t\pi}}\left(t+\frac{1}{a}\right)e^{-\beta_2 t}\right\}\Big],$$

$$P_2(y,t)=\left(\frac{1}{2}\right)\Big[\left(2t\sqrt{P_r\beta_2}+\sqrt{\frac{P_r}{\beta_2}}\right)\left(erfc\left(\sqrt{\beta_2 t}\right)-1\right)-2\sqrt{\frac{P_r}{t\pi}}e^{-\beta_2 t}\Big].$$

(ii) For isothermal plate

$$\tau=\left(\frac{R_1}{2}\right)\left[\left(\frac{1}{\sqrt{\beta_1}}+2t\sqrt{\beta_1}\right)\left(erfc\left(\sqrt{\beta_1 t}\right)-1\right)-2\sqrt{\frac{t}{\pi}}e^{-\beta_1 t}\right]+\left(\frac{\alpha}{2a}\right)\Big[e^{at}\left\{-2\sqrt{(\beta_1+a)}\left(erfc\left(\sqrt{(\beta_1+a)t}\right)-1\right)+2\sqrt{P_r(\beta_2+a)}\left(erfc\left(\sqrt{(\beta_2+a)t}\right)-1\right)\right\}+\left\{2\sqrt{\beta_1}\left(erfc\left(\sqrt{\beta_1 t}\right)-1\right)-2\sqrt{P_r\beta_2}\left(erfc\left(\sqrt{\beta_2 t}\right)-1\right)\right\}\Big]+\left(\frac{\gamma}{2b}\right)\Big[e^{bt}\left\{2\sqrt{(\beta_1+b)}\left(erfc\left(\sqrt{(\beta_1+b)t}\right)-1\right)-2\sqrt{S_c b}\left(erfc\left(\sqrt{bt}\right)-1\right)\right\}+\left\{-2\sqrt{\beta_1}\times\left(erfc\left(\sqrt{\beta_1 t}\right)-1\right)\right\}\Big], \quad (28)$$

$$N_u=\sqrt{\beta_2 P_r}\left(erfc\left(\sqrt{\beta_2 t}\right)-1\right)-\sqrt{\frac{P_r}{t\pi}}e^{-\beta_2 t}. \quad (29)$$

2.4 Sherwood Number

The expression for Sherwood number S_h, which is a measure of rate of mass transfer at the plate, is given by

$$S_h=-\sqrt{\frac{S_c}{t\pi}}. \quad (30)$$

Expression, presented by Eq. (30) depicts that Sherwood number increases on increasing Schimidt number S_c and decreases on increasing time. Since S_c presents relative strength of viscosity to molecular diffusivity of the fluid, S_c decreases on increasing molecular diffusivity. This implies that molecular diffusivity tends to reduce rate of mass transfer at the plate and there is a reduction in rate of mass transfer at the plate with the progress of time.

3. Results And Discussion

In order to study the influence of Hall current, rotation, radiation, heat absorption, thermal buoyancy force, solutal buoyancy force, mass diffusion and time on the flow-field, the numerical values of primary and secondary fluid velocities in the boundary layer region, computed from the analytical solutions, presented by Eqs. (20) and (25), are displayed graphically versus boundary layer coordinate y for various values of Hall current parameter m, rotation parameter K^2, radiation parameter R, heat absorption parameter ϕ, Grashof number G_r, solutal Grashof number G_c, Schmidt number S_c and time t, taking magnetic parameter $M=15$, permeability parameter $K_1=0.2$ and Prandtl number $P_r=0.71$ (ionized air) in Figs. 2 to 17. It is revealed from Figs. 2 to 17 that, for both ramped temperature and isothermal plates, primary fluid velocity u and secondary fluid velocity w attain a distinctive maximum value near the surface of the plate and then decrease properly on increasing boundary layer coordinate y to approach free stream value. Also the primary and secondary fluid velocities are faster in case of isothermal plate than that of ramped temperature plate. It is observed form Figs. 2 and 3 that, for both ramped temperature and isothermal plates, u

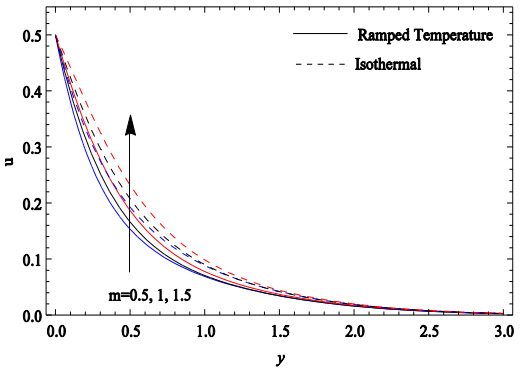

Fig. 2. Primary velocity profiles when $K^2=2, R=2, \phi=3, G_r=4, G_c=3, S_c=0.6$ and $t=0.5$.

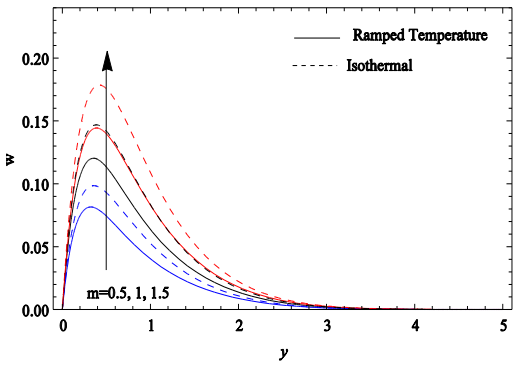

Fig. 3. Secondary velocity profiles when $K^2=2$, $R=2, \phi=3, G_r=4$, $G_c=3, S_c=0.6$ and $t=0.5$.

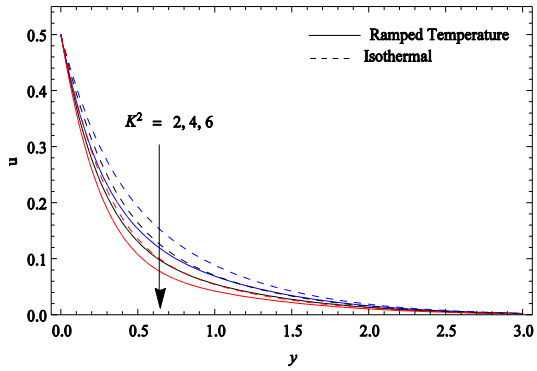

Fig. 4. Primary velocity profiles when $m = 0.5$, $R = 2, \phi = 3, G_r = 4, G_c = 3, S_c = 0.6$ and $t = 0.5$

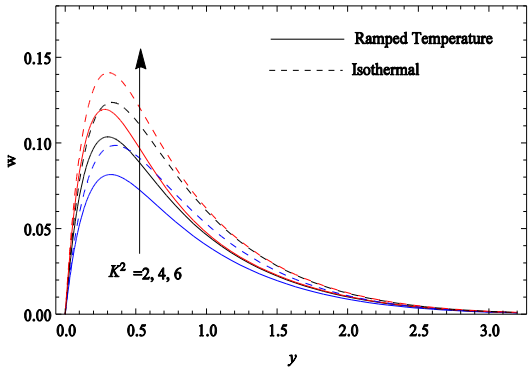

Fig. 5. Secondary velocity profiles when $m = 0.5$, $R = 2$, $\phi = 3$, $G_r = 4$, $G_c = 3$, $S_c = 0.6$ and $t = 0.5$.

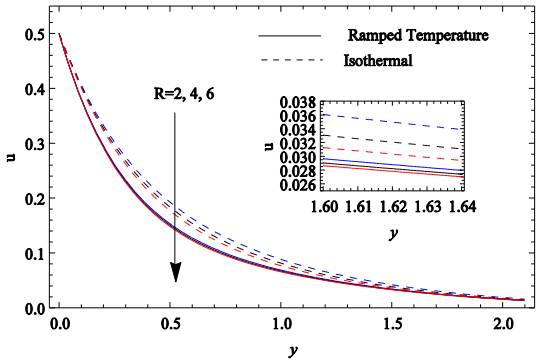

Fig. 6. Primary velocity profiles when $m = 0.5$, $K^2 = 2$, $\phi = 3, G_r = 4, G_c = 3, S_c = 0.6$ and $t = 0.5$

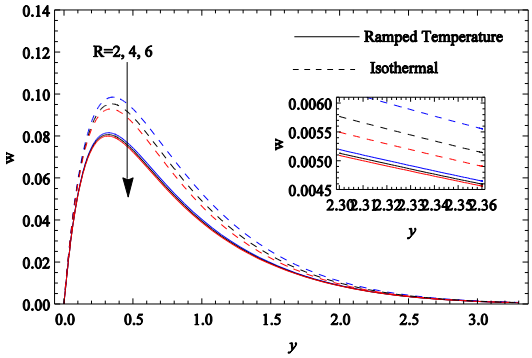

Fig. 7. Secondary velocity profiles when $m = 0.5$, $K^2 = 2$, $\phi = 3, G_r = 4, G_c = 3, S_c = 0.6$ and $t = 0.5$

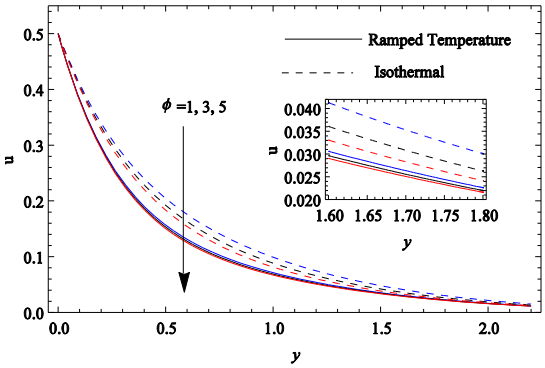

Fig. 8. Primary velocity profiles when $m = 0.5$, $K^2 = 2$, $R = 2$, $G_r = 4$, $G_c = 3$, $S_c = 0.6$ and $t = 0.5$.

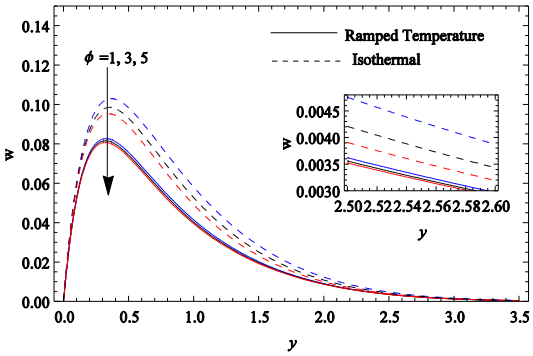

Fig. 9. Secondary velocity profiles when $m = 0.5$, $K^2 = 2$, $R = 2$, $G_r = 4$, $G_c = 3$, $S_c = 0.6$ and $t = 0.5$.

and w increase on increasing m. This implies that Hall current tends to accelerate primary and secondary fluid velocities for both ramped temperature and isothermal plates. This is due to the reason that Hall current induces secondary flow in the flow field.

It is revealed from Figs. 4 and 5 that u decreases on increasing K^2 whereas w increases on increasing K^2 for both ramped temperature and isothermal plates. This implies that rotation tends to retard the primary fluid velocity whereas it has a reverse effect on secondary fluid velocity for both ramped temperature and isothermal plates which is in agreement with the characteristics of Coriolis force which tends to suppress the primary flow for inducing the secondary flow. It is noticed from Figs. 6 to 9 that u and w decrease on increasing either R or ϕ for both ramped temperature and isothermal plates. This implies that radiation and heat absorption tend to retard the primary and secondary fluid velocities for both ramped temperature and isothermal plates. This is because radiation and heat absorption have tendency to reduce fluid temperature which is clearly evident from Figs. 18 and 19.

It is evident from Figs. 10 to 13 that u and w increase

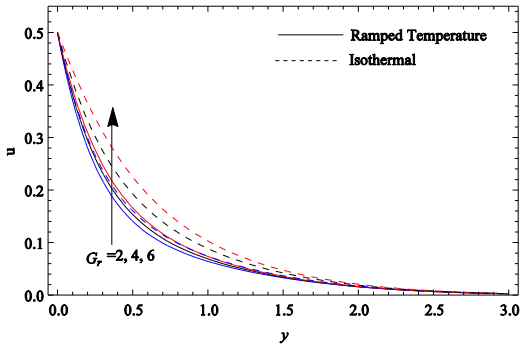

Fig. 10. Primary velocity profiles when $m = 0.5$, $K^2 = 2$, $R = 2$, $\phi = 3$, $G_c = 3$, $S_c = 0.6$ and $t = 0.5$.

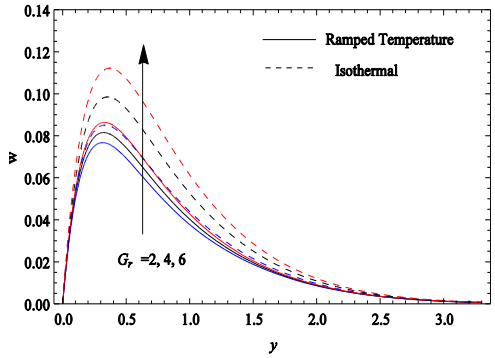

Fig. 11. Secondary velocity profiles when $m = 0.5$, $K^2 = 2$, $R = 2$, $\phi = 3$, $G_c = 3$, $S_c = 0.6$ and $t = 0.5$.

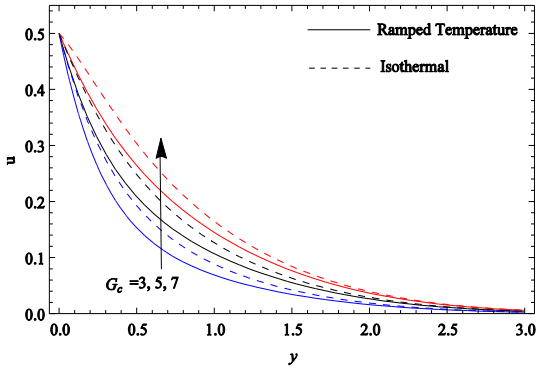

Fig. 12. Primary velocity profiles when $m = 0.5$, $K^2 = 2$, $R = 2$, $\phi = 3$, $G_r = 4$, $S_c = 0.6$ and $t = 0.5$.

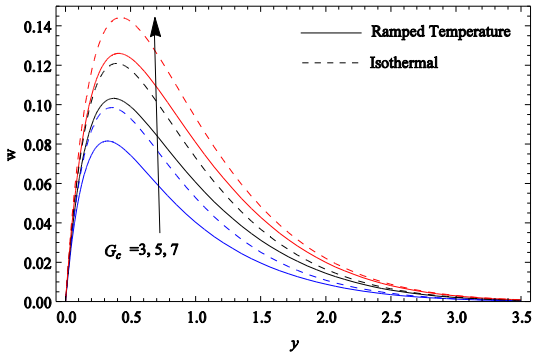

Fig. 13. Secondary velocity profiles when $m = 0.5$, $K^2 = 2$, $R = 2$, $\phi = 3$, $G_r = 4$, $S_c = 0.6$ and $t = 0.5$.

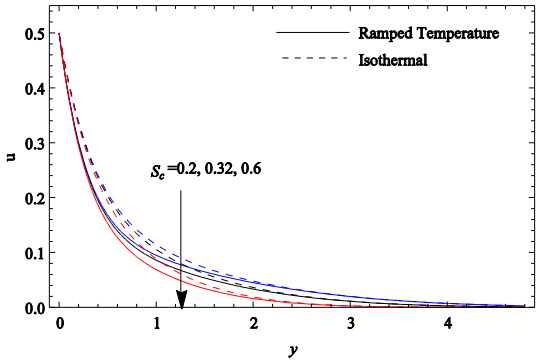

Fig. 14. Primary velocity profiles when $m = 0.5$, $K^2 = 2$, $R = 2$, $\phi = 3$, $G_r = 4$, $G_c = 3$ and $t = 0.5$.

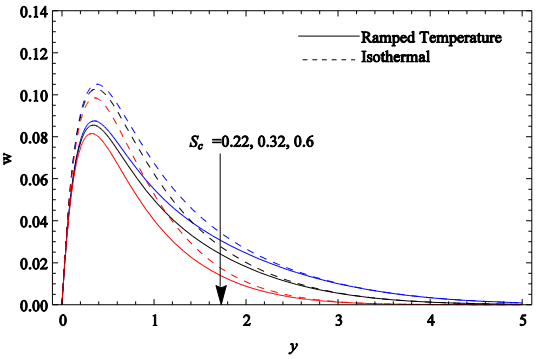

Fig. 15. Secondary velocity profiles when $m = 0.5$, $K^2 = 2$, $R = 2$, $\phi = 3$, $G_r = 4$, $G_c = 3$ and $t = 0.5$.

on increasing either G_r or G_c for both ramped temperature and isothermal plates. Physically, G_r presents relative strength of thermal buoyancy force to viscous force whereas G_c presents the relative strength of solutal buoyancy force to viscous force. G_r increases on increasing thermal buoyancy force and G_c increases on increasing solutal buoyancy force. This implies that thermal buoyancy force and concentration buoyancy force tend to accelerate the primary and secondary fluid velocities for both ramped temperature and isothermal plates. It is noticed from Figs. 14 and 15 that u and w decrease on increasing S_c for both ramped temperature and isothermal plates.

Since Schmidt number S_c is a measure of relative strength of viscosity to chemical molecular diffusivity. This implies that mass diffusion tends to accelerate the primary and secondary fluid velocities for both ramped temperature and isothermal plates. It is observed from Figs. 16 and 17 that u and w increase on increasing t for both ramped temperature and isothermal plates. This implies that primary and secondary fluid velocities are getting accelerated with the progress of time for both ramped temperature and isothermal plates. The numerical values for fluid temperature T computed from analytical solutions, presented by Eqs. (18) and (24), are displayed graphically versus boundary layer coordinate y in Figs. 18 to 20 for various values of heat absorption parameter ϕ, radiation parameter R and time t taking Prandtl number $P_r = 0.71$. It is

evident from Figs. 18 to 20 that fluid temperature T decreases on increasing either ϕ or R for both ramped temperature and isothermal plates whereas it increases on increasing t.

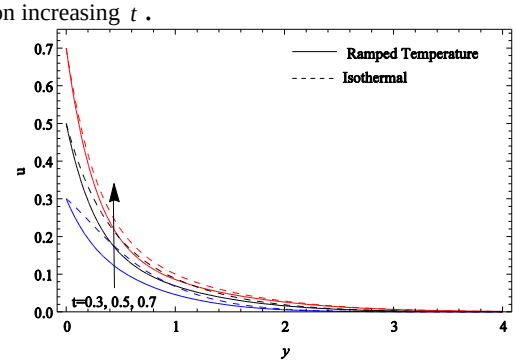

Fig. 16. Primary velocity profiles when $m = 0.5$, $K^2 = 2$, $R = 2$, $\phi = 3.$, $G_r = 4$, $G_c = 3$ and $S_c = 0.6$.

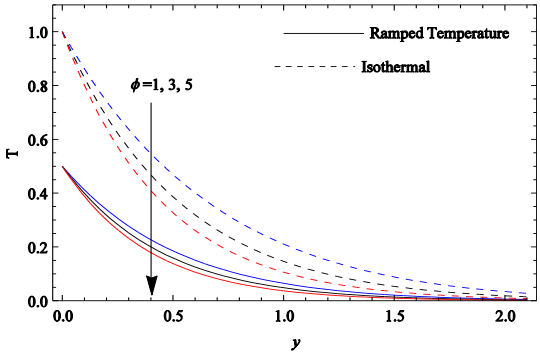

Fig. 18. Temperature profiles when $R = 2$ and $t = 0.5$.

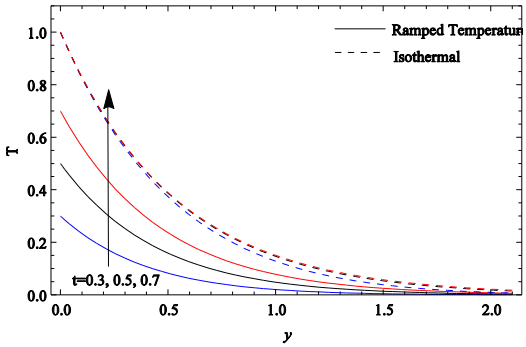

Fig. 20. Temperature profiles when $R = 2$ and $\phi = 3$.

This implies that, for both ramped temperature and isothermal plates, heat absorption and radiation have tendency to reduce fluid temperature. Fluid temperature is getting enhanced with the progress of time for both ramped temperature and isothermal plates. It is noticed from Figs. 18 to 20 that, for both ramped temperature and isothermal plates, fluid temperature is maximum at the surface of the plate and it decreases properly on increasing boundary layer coordinate y to attain free stream value. Also, fluid temperature is higher in case of isothermal plate than that of ramped temperature plate.

The numerical values of species concentration C, computed from the analytical solution, presented by Eq.

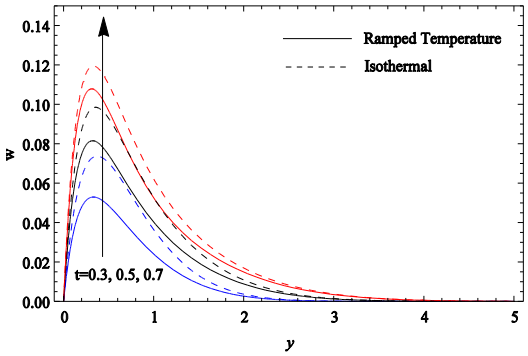

Fig. 17. Secondary velocity profiles when $m = 0.5$, $K^2 = 2$, $R = 2$, $\phi = 3.$, $G_r = 4$, $G_c = 3$ and $S_c = 0.6$.

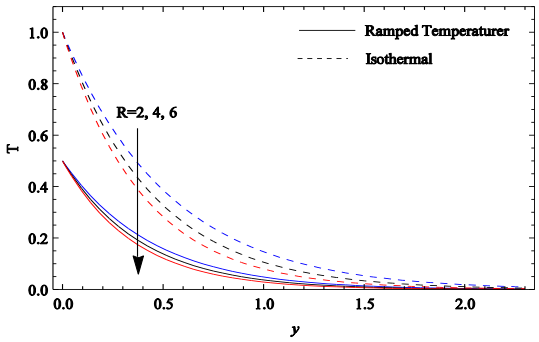

Fig. 19. Temperature profiles when $\phi = 3$ and $t = 0.5$.

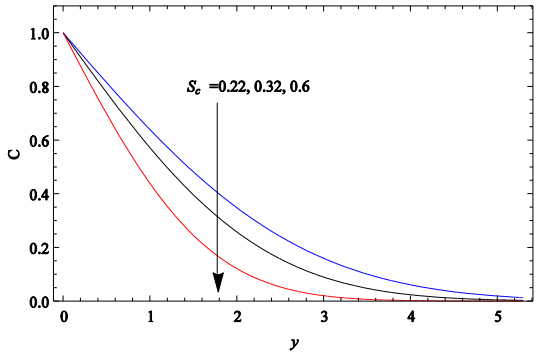

Fig. 21. Concentration profiles when $t = 0.5$.

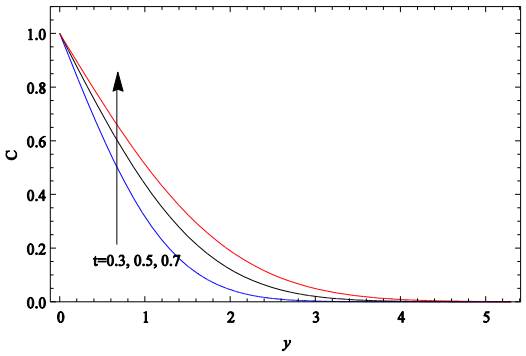

Fig. 22. Concentration profiles when $S_c = 0.6$.

(19), are presented graphically versus boundary layer coordinate y in Figs. 21 and 22 for various values of Schmidt number S_c and time t. It is evident from Figs. 21 and 22 that species concentration C decreases on increasing S_c whereas it increases on increasing t.

Table 1 Skin friction at ramped temperature plate when $G_r = 4$, $G_c = 3$, $\phi = 3$, $R = 2$, $S_c = 0.6$ and $t = 0.5$.

	$K^2 \downarrow\ m \rightarrow$	0.5	1	1.5
$-\tau_x$	2	1.3951	1.1343	0.9100
	4	1.4962	1.2806	1.0887
	6	1.6095	1.4281	1.2617
τ_z	2	0.7275	0.9572	1.0303
	4	0.9765	1.2081	1.2912
	6	1.1981	1.4227	1.5071

Table 2 Skin friction at isothermal plate when $G_r = 4$, $G_c = 3$, $\phi = 3$, $R = 2$, $S_c = 0.6$ and $t = 0.5$.

	$K^2 \downarrow\ m \rightarrow$	0.5	1	1.5
$-\tau_x$	2	0.9649	0.6291	0.3374
	4	0.9669	0.6329	0.3425
	6	0.9773	0.6515	0.3673
τ_z	2	0.7990	1.0619	1.1555
	4	1.0660	1.3276	1.4297
	6	1.2999	1.5503	1.6512

Table 3 Skin friction at ramped temperature plate when $m = 0.5$, $K^2 = 2$, $\phi = 3$, $R = 2$, $S_c = 0.6$ and $t = 0.5$.

	$G_c \downarrow\ G_r \rightarrow$	2	4	6
$-\tau_x$	3	1.5382	1.3951	1.2520
	5	1.1583	1.0518	0.8721
	7	0.7784	0.6353	0.4922
τ_z	3	0.7047	0.7275	0.7502
	5	0.7900	0.8128	0.8356
	7	0.8754	0.8982	0.9210

Table 4 Skin friction at isothermal plate when $m = 0.5$, $K^2 = 2$, $\phi = 3$, $R = 2$, $S_c = 0.6$ and $t = 0.5$.

	$G_c \downarrow\ G_r \rightarrow$	2	4	6
$-\tau_x$	3	1.3691	1.0568	0.7445
	5	0.9892	0.6769	0.3646
	7	0.6093	0.2970	0.0153
τ_z	3	0.7404	0.7990	0.8575
	5	0.8258	0.8843	0.9249
	7	0.9112	0.9697	1.0282

Table 5 Skin friction at ramped temperature plate when $m = 0.5$, $K^2 = 2$, $G_r = 4$, $G_c = 3$, $S_c = 0.6$ and $t = 0.5$.

	$\phi \downarrow\ R \rightarrow$	2	4	6
$-\tau_x$	1	1.3822	1.3951	1.4058
	3	1.3951	1.4058	1.4149
	5	1.4058	1.4149	1.4229
τ_z	1	0.7315	0.7275	0.7242
	3	0.7275	0.7242	0.7215
	5	0.7242	0.7215	0.7192

Table 6 Skin friction at isothermal plate when $m = 0.5$, $K^2 = 2$, $G_r = 4$, $G_c = 3$, $S_c = 0.6$ and $t = 0.5$.

	$\phi \downarrow\ R \rightarrow$	2	4	6
$-\tau_x$	1	1.0181	1.0570	1.0868
	3	1.0570	1.0870	1.1110
	5	1.0870	1.1110	1.1312
τ_z	1	0.8136	0.7990	0.7880
	3	0.7990	0.7880	0.7794
	5	0.7880	0.7793	0.7725

Table 7 Skin friction at ramped temperature plate when $m = 0.5$, $K^2 = 2$, $G_r = 4$, $G_c = 3$, $\phi = 3$ and $R = 2$.

	$S_c \downarrow\ t \rightarrow$	0.3	0.5	0.7
$-\tau_x$	0.22	0.6431	1.3571	2.0754
	0.32	0.6565	1.3673	2.0860
	0.6	0.6845	1.3889	2.1043
τ_z	0.22	0.4775	0.7458	1.0092
	0.32	0.4698	0.7398	1.0030
	0.6	0.4548	0.7275	0.9925

Table 8 Skin friction at isothermal plate when $m = 0.5$, $K^2 = 2$, $G_r = 4$, $G_c = 3$, $\phi = 3$ and $R = 2$.

	$S_c \downarrow\ t \rightarrow$	0.3	0.5	0.7
$-\tau_x$	0.22	0.1890	1.0250	1.8709
	0.32	0.2024	1.0351	1.8814
	0.6	0.2304	1.0570	1.8998
τ_z	0.22	0.5664	0.8173	1.0582
	0.32	0.5587	0.8113	1.052
	0.6	0.5437	0.7990	1.0415

This implies that mass diffusion tends to enhance species concentration and there is an enhancement in species concentration with the progress of time throughout the boundary layer region.

The numerical values of primary skin friction τ_x and secondary skin friction τ_z for both ramped temperature and isothermal plates, computed from the analytical expressions, presented by Eqs. (26) and (28), are presented in tabular form in Tables 1 to 8 for various values of K^2, m, G_r, G_c, ϕ, R, S_c and t taking $M = 15$, $K_1 = 0.2$ and $P_r = 0.71$ whereas those of Nusselt number N_u for both ramped temperature and isothermal plates, computed from analytical expressions, presented by Eqs. (27) and (29), are provided in Table 9 for different values of ϕ, R and t taking $P_r = 0.71$. It is noted from Tables 1 to 8 that the numerical values of primary skin friction for ramped temperature plate is higher than that for isothermal plate whereas the numerical values of secondary skin friction for ramped temperature plate is lower than that for isothermal plate. It is evident from Tables 1 to 8 that τ_x decreases on increasing m, G_r and G_c whereas it increases on increasing K^2, ϕ, R, S_c and t for both ramped temperature and isothermal plates. τ_z increases on increasing K^2, m, G_r, G_c and t whereas it decreases on increasing ϕ, R and S_c for both ramped temperature and isothermal plates.

Table 9 Nusselt number $-N_u$.

R	ϕ	t	Ramped Temperature	Isothermal plate
2	3	0.3	0.88457	1.92093
2	3	0.5	1.15702	1.89157
2	3	0.7	1.51219	1.88595
2	1	0.5	1.04197	1.48794
2	3	0.5	1.15702	1.89157
2	5	0.5	1.28383	2.23148
2	3	0.5	1.15702	1.89157
4	3	0.5	1.28383	2.23148
6	3	0.5	1.40804	2.52849

This implies that Hall current, thermal buoyancy force, solutal buoyancy force and mass diffusion tend to reduce primary skin friction whereas these agencies have reverse effect on secondary skin friction for both ramped temperature and isothermal plates. Rotation tends to enhance primary and secondary skin frictions for both ramped temperature and isothermal plates. Heat absorption and radiation tend to enhance primary skin friction whereas these agencies have reverse effect on secondary skin friction for both ramped temperature and isothermal plates. Primary and secondary skin frictions are getting enhanced for both ramped temperature and isothermal plates with the progress of time.

It is evident from Table 9 that Nusselt number N_u increases on increasing either ϕ or R for both ramped temperature and isothermal plates. On increasing time t, Nusselt number N_u increases for ramped temperature plate whereas it decreases for isothermal plate. This implies that, for both ramped temperature and isothermal plates, heat absorption and radiation tend to enhance rate of heat transfer at the plate. Rate of heat transfer at the plate is getting enhanced for ramped temperature plate whereas it is getting reduced for isothermal plate with the progress of time.

4. CONCLUSIONS

Present investigation deals with unsteady hydromagnetic natural convection heat and mass transfer flow with Hall current of a viscous, incompressible, electrically conducting, temperature dependent heat absorbing and optically thin heat radiating fluid past an accelerated moving vertical plate through fluid saturated porous medium in a rotating environment when temperature of the plate has a temporarily ramped profile.

Noteworthy results are summarized below:

- For both ramped temperature and isothermal plates:
  Hall current, thermal buoyancy force, solutal buoyancy force and mass diffusion tend to accelerate primary and secondary fluid velocities whereas heat absorption and radiation have reverse effect on it. Rotation tends to retard the primary fluid velocity whereas it has a reverse effect on secondary fluid velocity. Primary and secondary fluid velocities are getting accelerated with the progress of time. Heat absorption and radiation have tendency to reduce fluid temperature. There is an enhancement in fluid temperature with the progress of time.
- For both ramped temperature and isothermal plates:
  Hall current, thermal buoyancy force, solutal buoyancy force and mass diffusion tend to reduce primary skin friction whereas these agencies have reverse effect on secondary skin friction. Rotation tends to enhance primary and secondary skin frictions. Heat absorption and radiaton tend to enhance primary skin friction whereas these agencies have reverse effect on secondary skin friction. Primary and secondary skin frictions are getting enhanced with the progress of time.
- For both ramped temperature and isothermal plates, heat absorption and radiation tend to enhance rate of heat transfer at the plate. Rate of heat transfer at the plate is getting enhanced for ramped temperature plate whereas it is getting reduced for isothermal plate with the progress of time.

ACKNOWLEDGEMENT

Authors are grateful to the reviewers for their valuable comments and suggestions which helped them to improve the quality of the research paper.

REFERENCES

Aboeldahab, E. M. and E.M. E. Elbarbary (2001). Hall current effect on magnetohydrodynamic free convection flow past a semi-infinite vertical plate with mass transfer, *Int. J. Eng. Sci.*, 39, 1641-1652.

Azzam, G. E. A. (2002). Radiation effects on the MHD mixed free forced convective flow past a semi-infinite moving vertical plate for high temperature differences, *Phys. Scr.*, 66, 71-76.

Chamkha, A. J. (2000). Thermal radiation and buoyancy effects on hydromagnetic flow over an accelerating permeable surface with heat source or sink, *Int. J. Engng. Sci.*, 38, 1699-1712.

Chamkha, A. J. (2004). Unsteady MHD convective heat and mass transfer past a semi infinite vertical permeable moving plate with heat absorption, *Int. J. Engng. Sci.*, 42, 217-230.

Chamkha, A. J. and A.R. A. Khaled (2001). Similarity solutions for hydromagnetic simultaneous heat and mass transfer by natural convection from an inclined plate with internal heat generation or absorption, *Heat Mass Transfer*, 37,117-123.

Chen, C. H. (2004). Combined heat and mass transfer in MHD free convection from a vertical surface with Ohmic heating and viscous dissipation, *Int. J. Eng. Sci.*, 42, 699-713.

Cramer, K. R. and S. I. Pai (1973). Magnetofluid dynamics for Engineers and Applied physicists, *McGraw Hill Book Company, NY.*

Das, S. S., A. Satapathy, J. K. Das and J. P. Panda (2009). Mass transfer effects on MHD flow and heat transfer past a vertical porous plate through a porous medium under oscillatory suction and heat source, *Int. J. Heat Mass Transfer*, 52, 5962–5969.

England, W. G. and A. F. Emery (1969). Thermal radiation effects on the laminar free convection boundary layer of an absorbing gas, *J. Heat Transfer*, 91, 37-44.

Ghosh, S. K., O. A. Beg and M. Narahari (2013). A study of unsteady rotating hydromagnetic free and forced convection in a channel subject to forced oscillation under an oblique magnetic field, *J. Appl. Fluid Mech.*, 6, 213-227.

Hossain, M. A. and H. S. Takhar (1996). Radiation effects on mixed convection along a vertical plate with uniform surface temperature, *Heat Mass Transfer*, 31, 243-248.

Jha, B. K. and A. O. Ajibade (2009). Free convective flow of heat generating/absorbing fluid between vertical porous plates with periodic heat input, *Int. Comm. Heat Mass Transfer*, 36, 624-631.

Muthucumaraswamy, R., N. Dhanasekar and G. E. Prasad, (2013). Rotation effects on unsteady flow past an accelerated isothermal vertical plate with variable mass transfer in the presence of chemical reaction of first order, *J. Appl. Fluid Mech.*, 6, 485-490.

Nandkeolyar, R. and M. Das (2013). Unsteady MHD free convection flow of a heat absorbing dusty fluid past a flat plate with ramped wall temperature, *Afr. Mat.*, DOI 10.1007/s 13370-013-0151-9.

Nandkeolyar, R., G. S. Seth, O. D. Makinde, P. Sibanda and Md. S. Ansari (2013a). Unsteady hydromagnetic natural convection flow of a dusty fluid past an impulsively moving vertical plate with ramped temperature in the presence of thermal radiation, *ASME J. Appl. Mech.*, 80, 061003-(1-9).

Nandkeolyar, R., M. Das and P. Sibanda (2013b). Unsteady hydromagnetic heat and mass transfer flow of a heat radiating and chemically reactive fluid past a flat porous plate with ramped wall temperature, *Math. Prob. Engng.*, 2013, Article ID 381806.

Nandkeolyar, R., M Das and P. Sibanda (2013c). Exact solutions of unsteady MHD free convection in a heat absorbing fluid flow past a flat plate with ramped wall temperature, *Boundary Value Prob.*, 2013, 247.

Nanousis, N. (1992). Thermal diffusion effects on MHD free convective and mass transfer flow past a moving infinite vertical plate in a rotating fluid, *Astrophys. Space Sci.*, 919, 313-322.

Narahari, M., O. A. Bég and S. K. Ghosh (2011). Mathematical modelling of mass transfer and free convection current effects on unsteady viscous flow with ramped wall temperature, *World J. Mech.*, 1, 176-184.

Narayana, S. P. V., B. Venkateswarlu and S. Venkataramana (2013). Effects of Hall current and radiation absorption on MHD micropolar fluid in a rotating system, *Ain. Shams Eng. J.*, http://dx.doi.org/10.1016/j.asej.2013.02.002

Ogulu, A. and J. Prakash (2006). Heat transfer to unsteady magneto-hydrodynamic flow past an infinite moving vertical plate with variable suction, *Phys. Scr.*, 74, 232–239.

Patra, R. R., S. Das, R. N. Jana and S. K. Ghosh (2012). Transient approach to radiative heat transfer free convection flow with ramped wall temperature, *J. Appl. Fluid Mech.*, 5, 9-13.

Prakash, J., D. Bhanumathi, A.G.V. Kumar and S.V.K. Verma (2013). Diffusion-thermo and radiation effects on unsteady MHD flow through porous medium past an impulsively started infinite vertical plate with variable temperature and mass diffusion, *Transp. Por. Med.*, 96, 135-151.

Prasad, K. V., K. Vajravelu and A. Sujatha (2013). Influence of internal heat generation/absorption, thermal radiation, magnetic field, variable fluid property and viscous dissipation on heat transfer characteristics of a Maxwell fluid over a stretching sheet, *J. Appl. Fluid Mech.*, 6, 249-256.

Ramadan, H. and A. J. Chamkha (2004). Analytical solutions for hydromagnetic free convection of a particulate suspension from an inclined plate with heat absorption, *Int. J. Fluid Mech. Res.*, 27, 447-467.

Raptis, A. (2011). Free convective oscillatory flow and mass transfer past a porous plate in the presence of radiation for an optically thin fluid, *Thermal Sci.*,15, 849-857.

Raptis, A., C. Perdikis and A. Leontitsis (2003). Effects of radiation in an optically thin gray gas flowing past a vertical infinite plate in the presence of a magnetic field, *Heat Mass Trans.*, 39, 771-773.

Reddy, T. S., M. C. Raju and S. V. K. Varma (2013). Unsteady MHD radiative and chemically reactive free convection flow near a moving vertical plate in porous medium, *J. Appl. Fluid. Mech.*, 6, 443-451.

Saha, G., T. Sultana and S. Saha (2010). Effect of thermal radiation and heat generation on MHD flow past a uniformly heated vertical plate, *Desalination Water Treatment*, 16, 57-65.

Seddeek, M.A. (2001). Thermal radiation and buoyancy effects on MHD free convective heat generating flow over an accelerating permeable surface with

temperature-dependent viscosity, *Canad. J. Phys.*, 79, 725-732.

Seth, G. S., G. K. Mahato and S. Sarkar (2013a). Effects of Hall current and rotation on MHD natural convection flow past an impulsively moving vertical plate with ramped temperature in the presence of thermal diffusion with heat absorption, *Int. J. Energy Tech.* 5, 1–12.

Seth, G. S., G.K. Mahato, S. Sarkar and Md.S. Ansari (2012). Effects of Hall current on hydromagnetic natural convection flow of a heat absorbing fluid past an impulsively moving vertical plate with ramped temperature, *Int. J. Appl. Math. Res.*, 1, 462-486.

Seth, G. S., R. Nandkeolyar and Md. S. Ansari (2011). Effect of rotation on unsteady hydromagnetic natural convection flow past an impulsively moving vertical plate with ramped temperature in a porous medium with thermal diffusion and heat absorption, *Int. J. Appl. Math. Mech.*, 7, 52-69.

Seth, G. S., R. Nandkeolyar and Md. S. Ansari (2013b). Effects of thermal radiation and rotation on unsteady hydromagnetic free convection flow past an impulsively moving vertical plate with ramped temperature in a porous medium, *J. Appl. Fluid Mech.* 6, 27-38.

Singh, A. K. (1983). MHD free convection flow in the Stokes problem for a vertical porous plate in a rotating system, *Astrophys. Space Sci*. 95, 283-289.

Singh, N.P., A.K. Singh and H. Singh (2010). Mixed convection flow past a porous vertical plate bounded by a porous medium in a rotating system in the presence of a magnetic field, *J. Porous Media*, 13, 623-633.

Sparrow, E. M. and R. D. Cess (1961). Temperature dependent heat sources or sinks in a stagnation point flow, *Appl. Sci. Res.*, 10, 185-197.

Sutton, G. W. and A. Sherman (1965). Engineering magnetohydrodynamics, *McGraw-Hill*, *New York.*